ChemSusChem

Supporting Information

Optimising Low Temperature Pyrolysis of Mesoporous Alginate-Derived Starbon® for Selective Heavy Metal Adsorption

Nicholas Garland,* Ross Gordon, Con Robert McElroy, Alison Parkin, and Duncan MacQuarrie*

Electronic Supplementary Information (ESI)

Optimising Low Temperature Pyrolysis of Mesoporous Alginate-Derived Materials for Base Metal Adsorption

Nicholas Garland,[a] Ross Gordon, [b] Con Robert McElroy,[c] Alison Parkin[a] and Duncan MacQuarrie[a]

[a] Department of Chemistry, University of York, York, YO10 5DD, UK

[b] Johnson Matthey Technology Centre, Sonning Common, Reading, RG4 9NH, UK

[c] School of Chemistry, University of Lincoln, Lincoln, LN6 7TS

Table of Contents

Photographs of A000, A200, A250 and A300

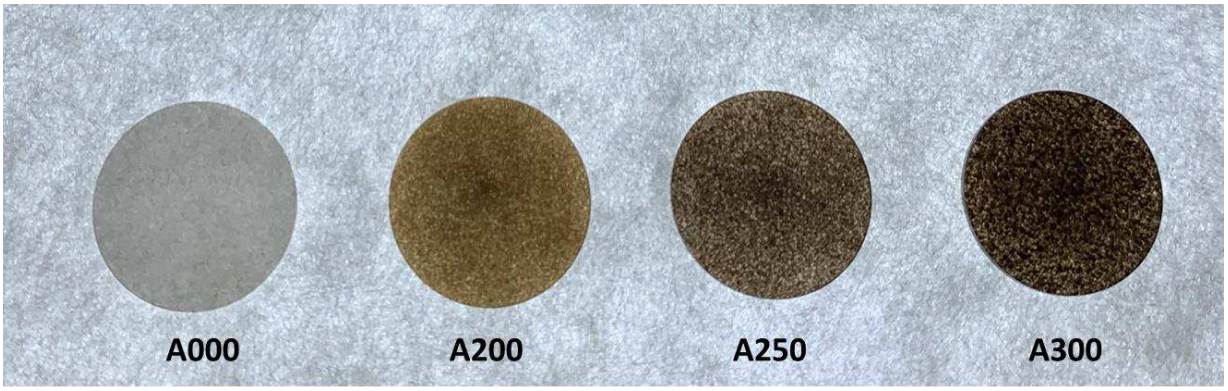

Figure S 1. Photographs of A000, A200, A250 and A300 in KBr (as prepared for transmission IR)

EDS elemental analysis

The elemental composition of all carbon materials was determined by SEM-EDS (JEOL 7800F Prime SEM) equipped with dual Oxford Instruments large area solid state detectors for energy dispersive X-ray spectroscopy. Atom % was averaged over 4 sites per sample. Prior to imaging, materials were coated with 6 nm Pt/Pd to prevent charge build up.

Table S 1. Elemental compositions of A000, A200, A250 and A300 as determined by SEM-EDS and expressed as atom %.

Material	Elemental composition / atom %					C:O
	C	O	Ca	Na	S	
A300	77.9	21.3	0.6	0.1	0.0	3.66
A250	72.2	26.4	0.3	0.0	0.1	2.73
A200	67.5	31.9	0.5	0.0	0.1	2.16
A000	54.5	44.9	0.4	0.0	0.1	1.21

CHN(O) elemental analysis

CHN analysis was conducted by Exeter Analytical using a CE440 CHN Elemental Analyser. Oxygen content was determined as the remaining wt% after C, H and N were subtracted (on the basis that inorganic content was less than 1% for all materials).

Table S 2. Elemental composition of A000, A200, A250 and A300 determined by CHN analysis.

Material	**Elemental composition / weight %**			
	C	**H**	**N**	**O**
A000	37.3	4.9	0.1	57.7
A200	49.7	4.3	0.1	45.9
A250	58.6	3.6	0.2	37.6
A300	62.5	3.2	0.2	34.1

Thermal analysis

Thermal analysis was conducted on a Netzsch STA 409 CD Simultaneous Thermal Analyser under flow of nitrogen (100 cm^3 min^{-1}). Ca. 100 mg of A000 was heated to 150 °C at 10 ° min^{-1}, followed by heating to 300 °C at 1 ° min^{-1}. Mass loss during pyrolysis to 0, 200, 250 and 300 °C are recorded in Table S 3 in addition to the mass lost due to washing with HCl and then water after pyrolysis.

Table S 3. Mass lost during pyrolysis to 0, 200, 250 and 300 °C, mass loss due to washing of the materials after pyrolysis and the total mass remaining after pyrolysis and washing of each material.

Material	% Mass loss (pyrolysis)	% Mass loss (washing)	Remaining mass (% of original mass)
A000	0.0	30.8	69.2
A200	27.1	26.5	53.6
A250	54.4	2.6	44.4
A300	62.5	1.9	36.8

Thermal gravimetry-gas chromatography-mass spectrometry

TG-GC-MS analysis was conducted using a Netzsch STA 449 Simultaneous Thermal Analyser coupled with Aglient 890 GC fitted with an Agilent 5977B GC-MS detector. The transfer line and valve box were heated to 300 °C and helium was used as a carrier gas. Ca. 15 mg A000 was heated to 300 °C at 10 ° min^{-1}.

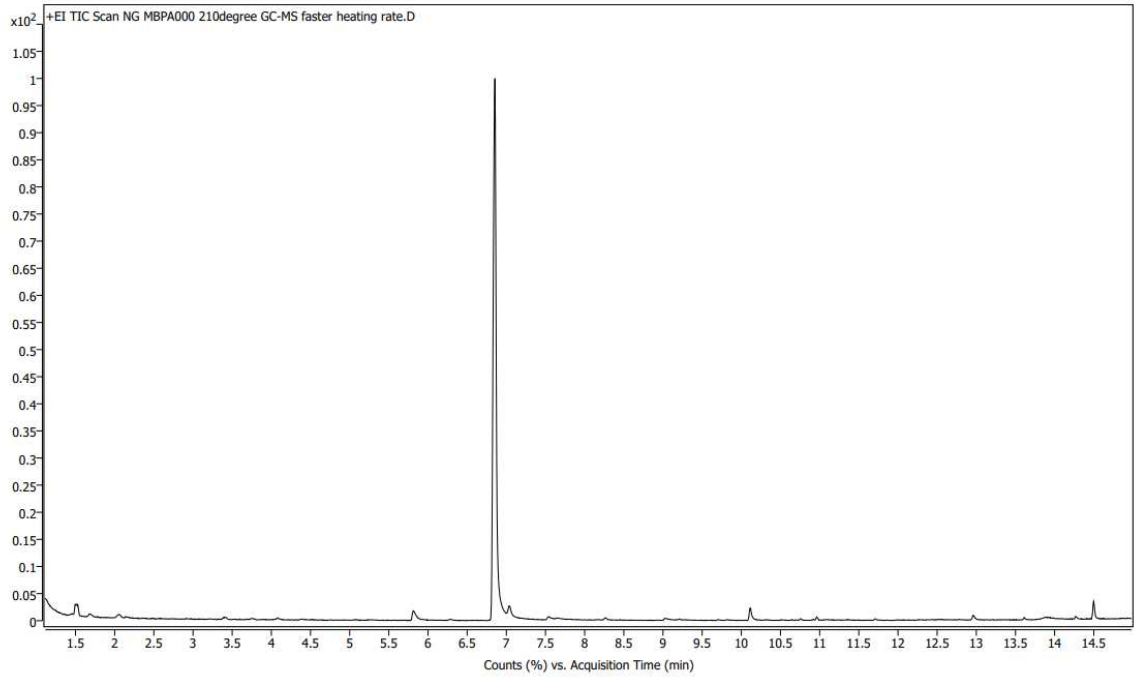

Figure S 2. Gas chromatogram of species evolved during pyrolysis of A000, at 210 °C.

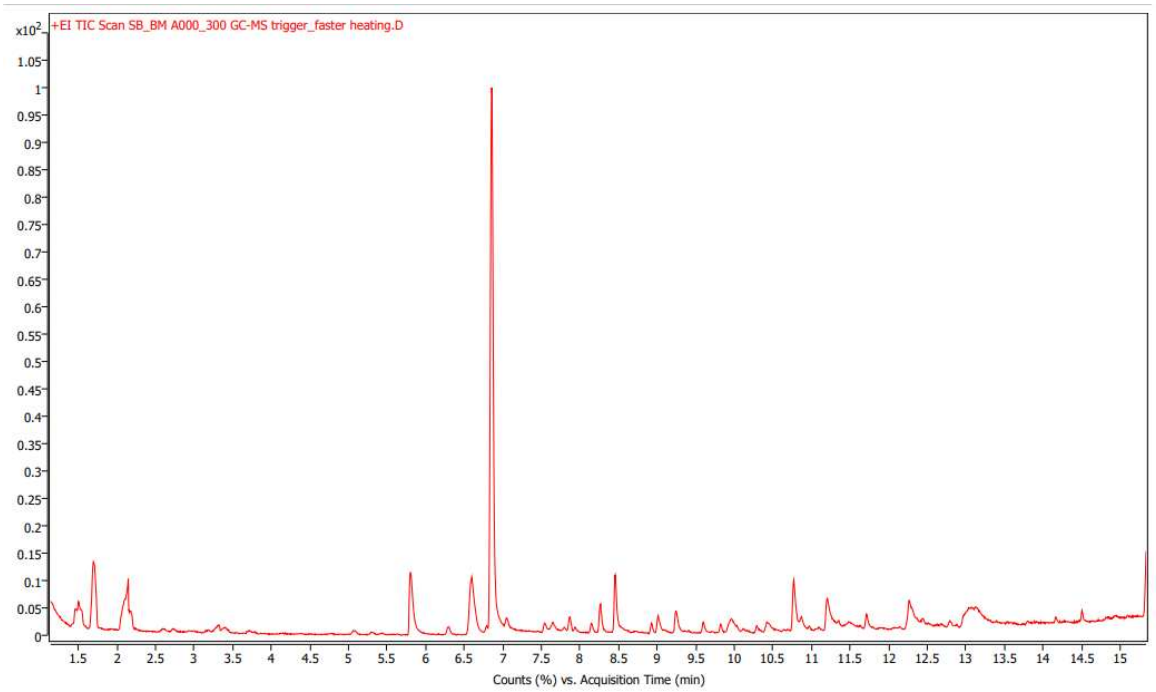

Figure S 3. Gas chromatogram of species evolved during pyrolysis of A000, at 300 °C.

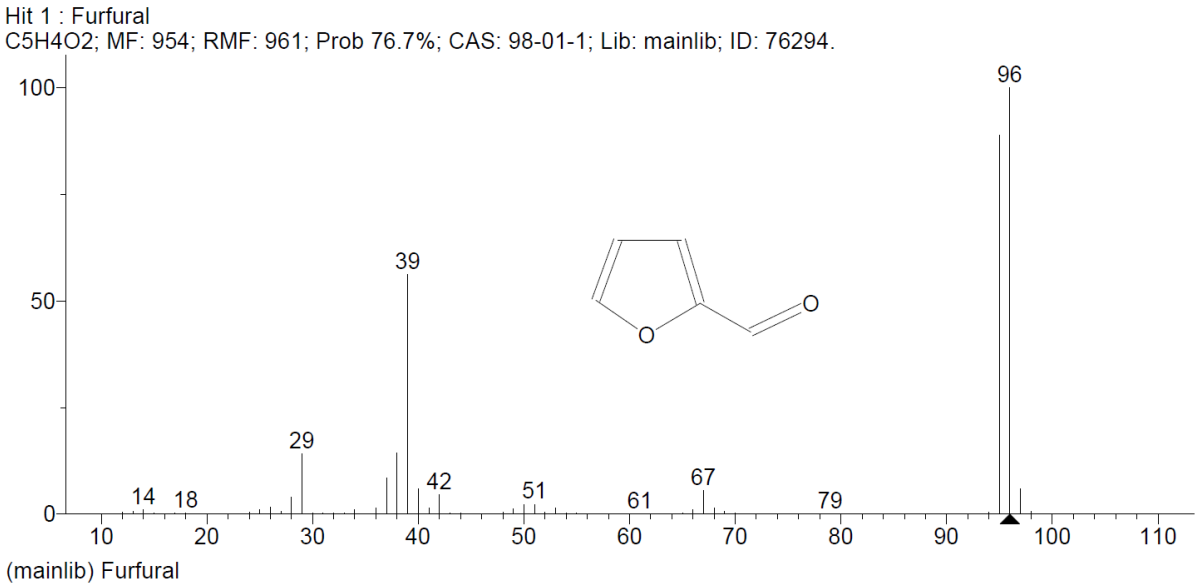

Figure S 4. Mass spectrum of species A (furfural), acquisition time 6.9 minutes

SEM

Micrographs were obtained on a JEOL 7800F Prime scanning electron microscope using an off-axis Everhart-Thornley lower electron detector (LED) at 5 keV and a working distance of 10 mm. Prior to imaging, materials were coated with 6 nm Pt/Pd to prevent charge build up.

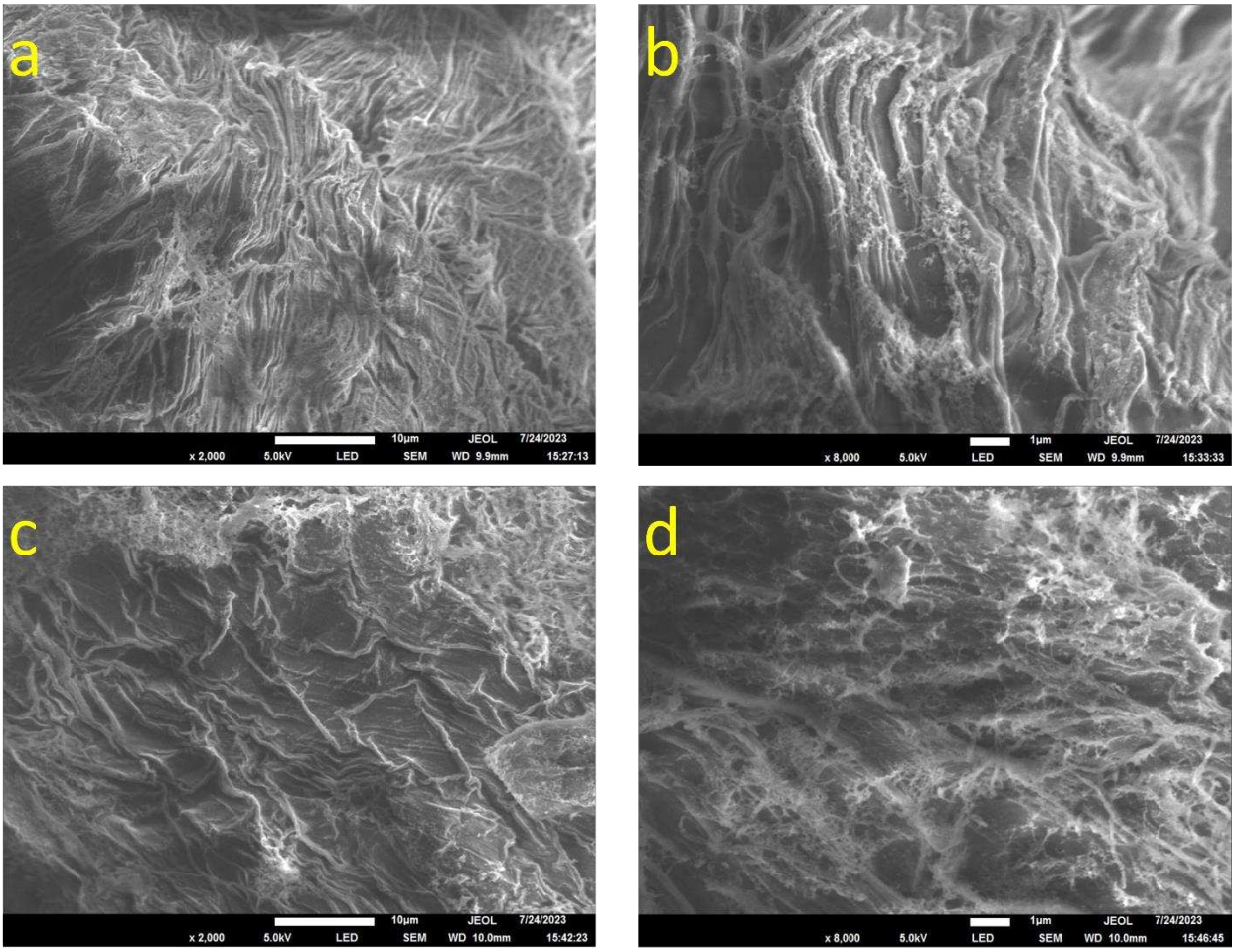

Figure S 5. SEM images of a) A000 x2000, b) A000 x8000, c) A200 x2000, d) A200 x8000

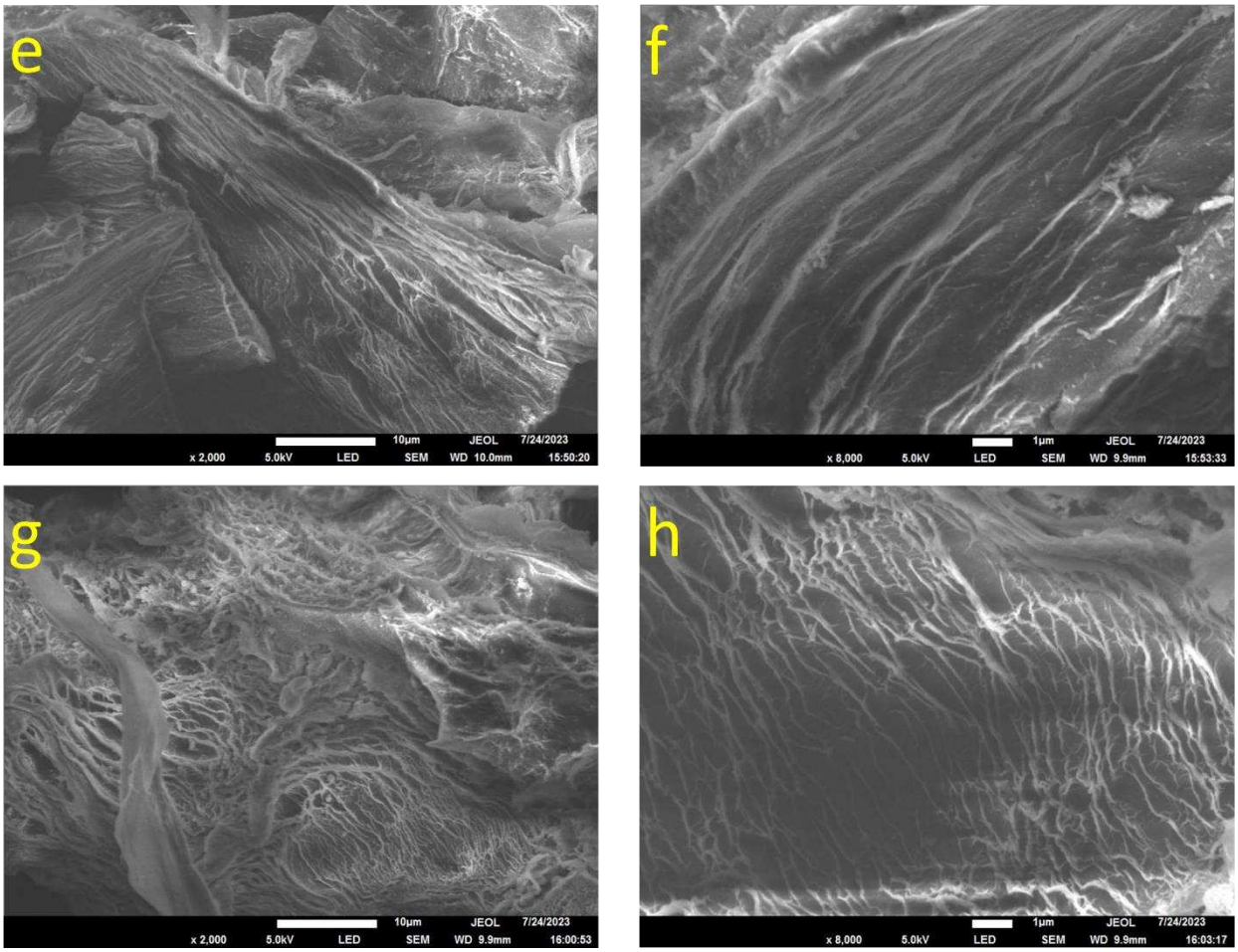

Figure S 6. SEM images of e) A250 x2000, f) A250 x8000, g) A300 x2000 and h) A300 x8000

Porosimetry

The textural properties of A000-300 were determined by N_2-sorption porosimetry using a Micrometrics ASAP 2020 volumetric adsorption analyser at 77 K. Prior to analysis, A300, A250 and A200 (~0.15 g) were degassed at 150 °C and 50 µm Hg for 4 hours. To prevent chemical decomposition, and subsequent textural change, A000 was degassed at 75 °C and 50 µm Hg until the mass of the sample remained constant for 5 hours (15 hours total), indicating that the sample had been effectively degassed. Total surface area (S_{BET}) was determined using the BET model, mesopore volume (V_{Meso}) was estimated using the Barrett-Joyner-Halenda (BJH) desorption method, micropore volume (V_{Micro}) was determined using t-plot equation. Materials were analysed prior to de-ashing so that pore structure was not destroyed by the subsequent drying process.

Table S 4. BET surface area, BJH mesopore volume and t-plot micropore volume of A000, A200, A250 and A300 determined by N_2-sorption porosimetry.

Carbon	BET surface area ($m^2\ g^{-1}$)	BJH mesopore volume ($cm^3\ g^{-1}$)	t-plot micropore volume ($cm^3\ g^{-1}$)	%micro
A000	286	1.547	0.009	0.58
A200	157	0.943	0	0.00
A250	205	0.912	0.002	0.22
A300	297	0.81	0.032	3.80
A300*	7	0.04	0.001	2.44

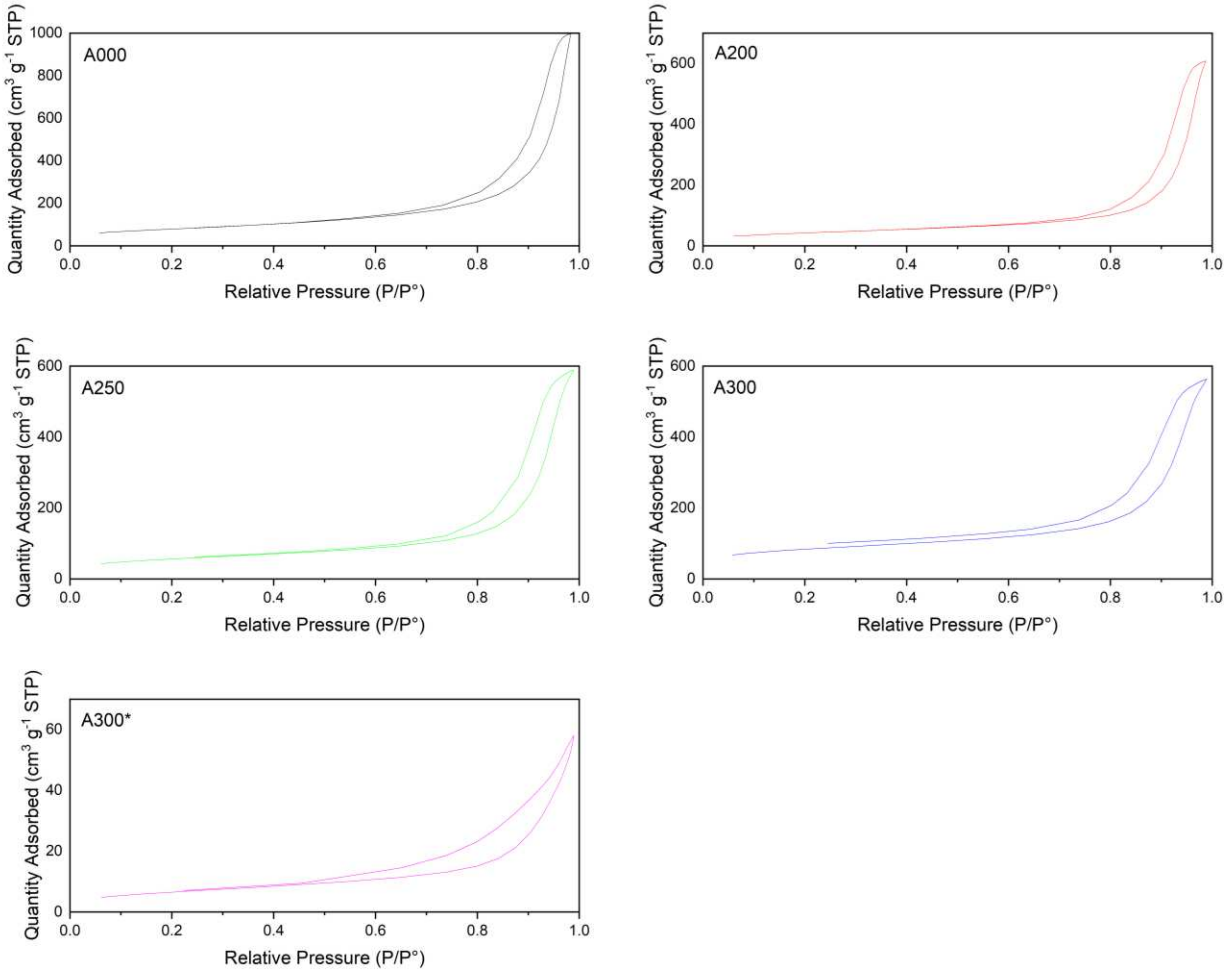

Figure S 7. N_2-sorption isotherms of A000, A200, A250, A300 and A300*.

Solid state ^{13}C MAS NMR

Solid state NMR was run by the advanced analytical team at Johnson Matthey Technology Centre. SS NMR spectra were acquired at a static magnetic field strength of 14.1 T (ν0(1H) = 600 MHz) on a Bruker Avance Neo console using TopSpin 4.0 software. For ^{13}C, the probe was tuned to 150.94 MHz and referenced to alanine CH_3 at 20.5 ppm. Powdered samples were packed into MAS rotors spun using room-temperature purified compressed air. The total experiment time to acquire these spectra was 11 hours.

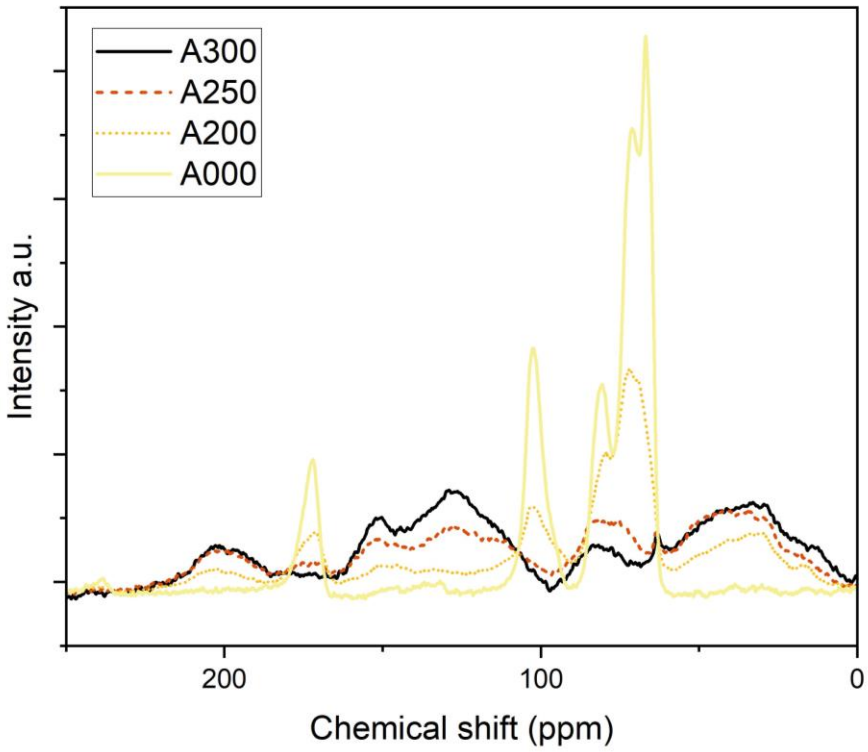

Figure S 8. Solid state ^{13}C NMR of A000, A200, A250 and A300

Adsorption Kinetics

The kinetics of copper adsorption were determined for A000, A250 and A300 using 0.16 g l^{-1} $CuCl_2$ solution at pH 4. 0.6 g of each material (dry) was added to 100 mL of copper solution and stirred with 1 mL aliquots taken at ca. 1, 3, 9, 30, 120, 1000 and 5000 minutes. Aliquots were diluted 20x in 2M HCl and the concentration of copper determined by UV-visible spectroscopy. The fraction of copper adsorbed from solution over time has been plotted in Figure S 9. After copper adsorption by A300 was complete, copper was removed by washing with 0.5M H_2SO_4 before the material was reused for adsorption.

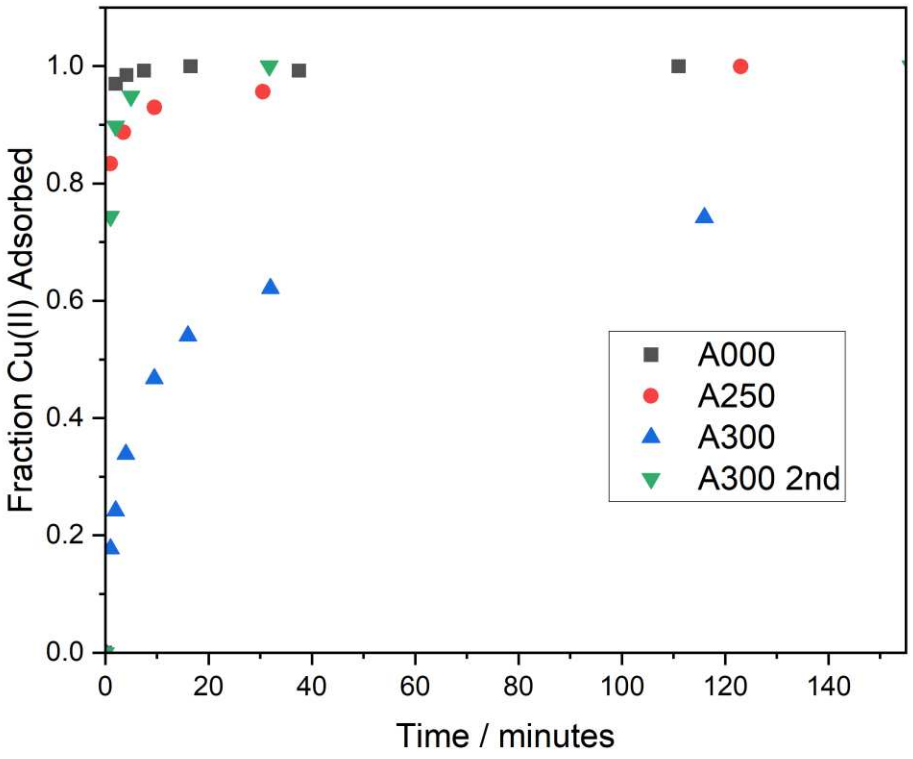

Figure S 9. Kinetics of copper adsorption by A000, A250 and A300. Two successive adsorption cycles were compared for A300 (A300 2nd).

The rate of copper adsorption by A300 was significantly faster during the second adsorption. It is suggested that the initially slow adsorption of copper by fresh A300 is limited by the reduced wettability of the more aliphatic A300 material. After adsorption/desorption of copper, the A300 material was not dried before being reused and as a result adsorption was faster. After wetting, we have found that in all cases adsorption is complete within 30 minutes.